NANO LETTERS

Letter

pubs.acs.org/NanoLett

Superior Conductive Solid-like Electrolytes: Nanoconfining Liquids within the Hollow Structures

Jinshui Zhang,[†] Ying Bai,[†,▽] Xiao-Guang Sun,[†] Yunchao Li,[†,#] Bingkun Guo,[∥] Jihua Chen,[‡] Gabriel M. Veith,[§] Dale K. Hensley,[‡] Mariappan Parans Paranthaman,[†,#] John B. Goodenough,[∥] and Sheng Dai*[,†,⊥]

[†]Chemical Sciences Division, [‡]Center for Nanophase Materials Sciences Division and [§]Materials Science and Technology Division, Oak Ridge National Laboratory, Oak Ridge, Tennessee 37831, United States

[∥]Texas Materials Institute, The University of Texas at Austin, Austin, Texas 78712, United States

[⊥]Department of Chemistry and [#]The Bredesen Center for Interdisciplinary Research and Graduate Education, University of Tennessee, Knoxville, Tennessee 37996, United States

[▽]Key Laboratory of Photovoltaic Materials of Henan Province and School of Physics and Electronics, Henan University, Kaifeng 475004, People's Republic of China

Supporting Information

ABSTRACT: The growth and proliferation of lithium (Li) dendrites during cell recharge are currently unavoidable, which seriously hinders the development and application of rechargeable Li metal batteries. Solid electrolytes with robust mechanical modulus are regarded as a promising approach to overcome the dendrite problems. However, their room-temperature ionic conductivities are usually too low to reach the level required for normal battery operation. Here, a class of novel solid electrolytes with liquid-like room-temperature ionic conductivities (>1 mS cm^{-1}) has been successfully synthesized by taking advantage of the unique nanoarchitectures of hollow silica (HS) spheres to confine liquid electrolytes in hollow space to afford high conductivities (2.5 mS cm^{-1}). In a symmetric lithium/lithium cell, the solid-like electrolytes demonstrate a robust performance against the Li dendrite problem, preventing the cell from short circuiting at current densities ranging from 0.16 to 0.32 mA cm^{-2} over an extended period of time. Moreover, the high flexibility and compatibility of HS nanoarchitectures, in principle, enables broad tunability to choose desired liquids for the fabrication of other kinds of solid-like electrolytes, such as those containing Na^+, Mg^{2+}, or Al^{3+} as conductive media, providing a useful alternative strategy for the development of next generation rechargeable batteries.

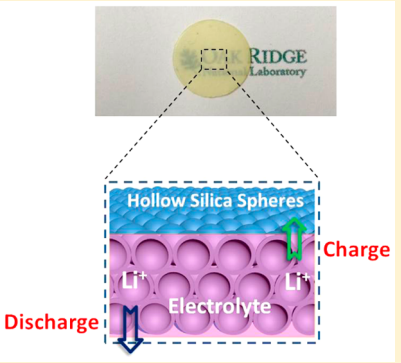

KEYWORDS: *Li dendrite, solid-like electrolyte, superior conductivity, hollow nanoarchitecture, nanoconfinement*

The application of Li−metal anodes for rechargeable batteries would be key in enabling technology for higher energy density Li-ion batteries as well as advanced chemistries such as lithium−sulfur and lithium−air systems.[5−9] This is because Li metal has a high theoretical capacity (3860 mAh g^{-1}), low density (0.59 g cm^{-3}), and the lowest negative electrochemical potential (−3.04 V vs standard hydrogen electrode (SHE)).[1−4] Despite the obvious benefits of Li−metal use in commercial and research cells, it is limited by the electrolyte instability and dendrite formation that result in serious safety problems.[3,7] For example, the nonuniformly deposited Li during cell recharge often results in the formation and proliferation of unavoidable dendrites, which sprout from the surface of the anode and spread like kudzu across the electrolyte/separator until they reach the cathode.[10−12] When an electrical current is passing through these dendrites, an internal short-circuit of the battery happens, causing the thermal runaway of the cells and in some instances even catching fire. The development of advanced electrochemical materials (electrode, electrolyte, and a separator) and the improved control of Li plating therefore is considered as a fundamental requirement toward the long-term operation of Li metal batteries.[11−16]

Solid Li ionic conductors, such as polymer, glass, and crystalline solids, are currently being widely investigated as candidate electrolytes of Li metal batteries, owing to their inherent advantages in terms of safety and device fabrication.[17−21] For example, solid electrolytes with mechanical modulus above Li metal can functionalize as rigid barriers to efficiently prevent the dendrites from crossing the interelectrode space, thus avoiding the battery from short-circuiting.[18−21] However, their ionic conductivities at room temperature are typically more than an order of magnitude too low to reach the level of normal battery operation.[18,22] In contrast,

Received: February 24, 2015
Revised: April 3, 2015
Published: April 6, 2015

DOI: 10.1021/acs.nanolett.5b00739
Nano Lett. 2015, 15, 3398−3402

Scheme 1. Illustration of the Synthetic Processing of the HS-film(A) Electrolytes

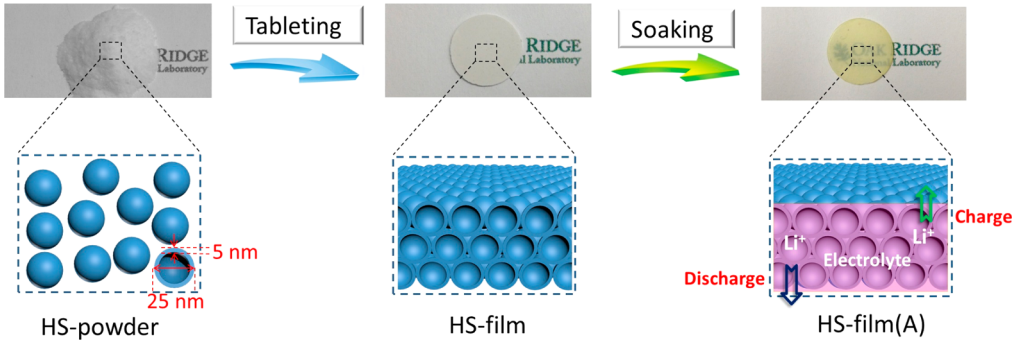

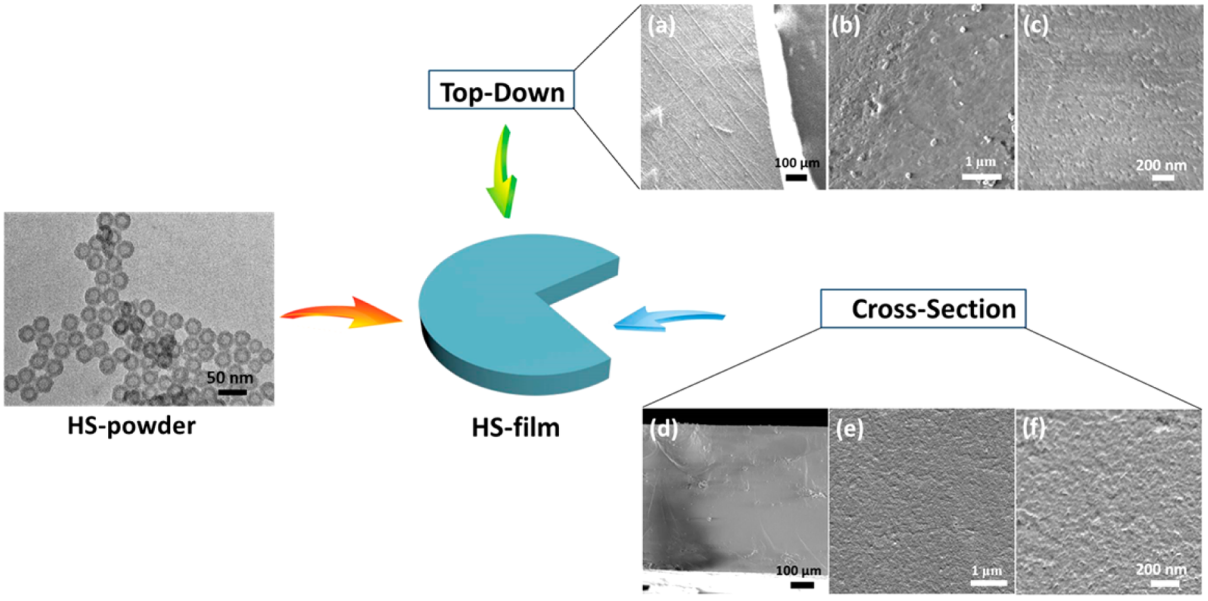

Figure 1. Typical SEM images collected for the HS-film.

organic liquid electrolytes feature very fast ionic transport properties ($>10^{-2}$ S cm^{-1}) but introduce the obvious flammability of carbonate solvents.[19]

We have been interested in a strategy to combine the benefits of liquid electrolytes (conduction) with the rigidity of a solid electrolyte. In principle, it is easy to combine the advantages both from solid electrolytes and liquid electrolytes in one material that has a solid-like mechanical modulus for dendrites blocking and liquid-like room-temperature ionic conductivities for Li^+ transport. Very recently, work along this direction has been carried out by the Archer group and our group in which polymer-based nanocomposites are used as the host for the loading of liquid electrolytes, including PVDF-HFP/Al_2O_3, PEO/Al_2O_3, and PVDF-HFP/PVP/Sb_2O_3.[23−25] As expected, these nanocomposites demonstrate a good mechanical strength to overcome the dendrite problems, providing an alternative approach to fabricate robust electrolytes. However, their nanostructures are less controllable with relatively porous frameworks, which may allow the dendrite to pass through causing a short. Hence, further nanoengineering of solid-like electrolytes with well-defined porous nanoarchitectures is of high significance.

One material that could advance us toward functional hybrid materials are hollow nanostructures with accessible inner space that could trap molecules or mediate diffusion.[26−28] One example is the hollow silica (HS) nanospheres where microporous silica shells can function as molecular sieves to size-selective catalyze allylic oxidation,[29] while their empty cavities can function as free-pathways to enhance gas transport through density liquid-like polymeric matrix for gas separation.[30] In addition, the HS nanospheres can be further employed as nanovehicles for drug delivery by taking advantage of their microporous shells for drug release and their empty cavities for drug loading.[31] Clearly, the application of HS nanospheres are closely dependent on their nanoarchitectures, and more additional functionality could be engineered by further optimizing their nanostructures.[26,27] We believe it would be possible to exploit the HS nanospheres as building blocks for the construction of mechanics-strong scaffolds for liquid-state electrolyte loading with the purpose to confine well organic liquid within inner space but impeding-free for Li^+ transport.

Herein, a class of solid electrolytes with liquid-like room-temperature ionic conductivities is facilely fabricated starting from HS nanospheres (Scheme 1). To better shape the nanoparticles as films via close-packing under high pressure, HS nanospheres with a diameter of ca. 25 nm and shell thickness of ca. 5 nm are synthesized and chosen as the building blocks, because their rather small particle sizes can afford enough mechanical stability against extrusion.[32,33] In addition, decreas-

DOI: 10.1021/acs.nanolett.5b00739
Nano Lett. 2015, 15, 3398−3402

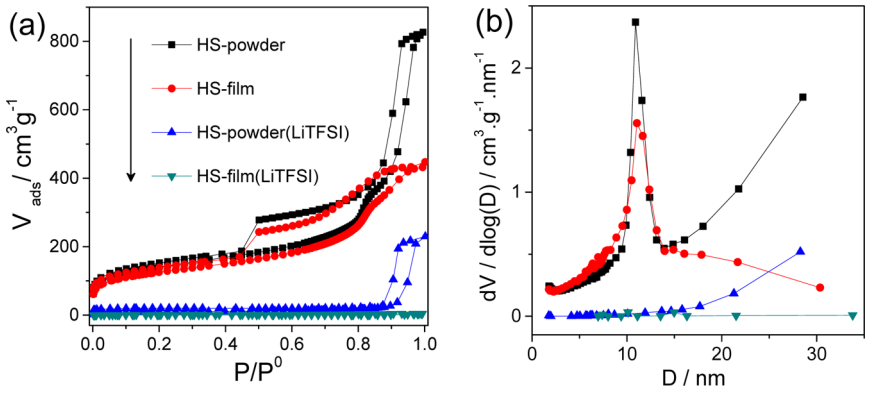

Figure 2. N_2-sorption isotherms (a) and BJH pore size distribution (b) of HS derived samples.

ing the particle size of HS will reduce the interparticle voids in the HS arrays facilitating the fabrication of dense films that could confine organic liquids in the pores and prevent the dendrites from crossing the interelectrode space. Experimentally, the HS-based film (HS-film) is prepared by molding of HS powder (HS-powder) in a stainless steel holder with an inner diameter of 12 mm under the pressure as high as 7 G Pa, and the thicknesses of the films is controllably adjusted by varying the weight of HS-powder. To facilitate the inclusion of the liquid electrolytes in hollow structures, the as-prepared HS-film is evacuated at 200 °C for 24 h to extract water and air previously trapped in HS spheres. After a sufficient soak in the selected liquid electrolyte, for example, $LiPF_6$ ethylene carbonate,dimethyl carbonate, the resultant film (denoted as HS-film(A), A corresponding to the abbreviation of selected liquid-state electrolyte) is transferred to a filter paper for the removal of residual solution on surfaces. The loading amount of liquids confined in HS-film is calculated from the mass difference of the film before and after soaking. Detailed information about the synthetic procedure is provided in the Experimental Section (see Supporting Information).

The surface morphologies and the local-packing of the nanoparticle arrays in HS-film are carefully examined by field emission scanning electron microscopy (SEM). In the top-down SEM images (Figure 1a−c), the individual nanospheres are closely squeezed together as a free-standing film in dense packing. In principle, such HS-film can function as a mechanics-strong separator in a cell system to block the Li dendrites during charge−discharge cycling because of the higher mechanical modulus of SiO_2 over Li metal.[23,34] The cross-section morphologies of HS-film are imaged in Figure 1d−f in which typical patterns resulting from particle stacking are observed. The large interparticle space present in HS-powder is evidently reduced by high-pressure extrusion, which is of great importance for the fabrication of the electrolyte, because the voids between neighboring nanospheres are too big for Li^+ transport. For example, the ionic conductivity of nondensified HS-powder that is fully soaked with the liquid electrolyte is measured as low as 10^{-7} S cm^{-1}. This poor conductivity can be greatly enhanced by just applying force to decrease the interparticle voids. Furthermore, the well-preserved hollow nanoarchitectures in the HS-film is clearly demonstrated by the enlarged SEM and transmission electron microscopy (TEM) images. In Supporting Information Figure S1 and S2, well-defined nanospheres are clearly observed without any deformation, and the hollow structure is still preserved in the HS-film. This finding is rather important, which indicates that the HS nanospheres are robust enough not to distort under pressures up to 7 GPa, keeping their morphologies and inner porosity.

The nanotextural structure of the HS-film and the HS-powder is characterized by N_2-sorption isotherms and the corresponding Barrett−Joyner−Halenda (BJH) pore-size distributions. In Figure 2a, a significant decrease of N_2 uptake in the region of relative pressure (P/P^0) above 0.85 is clearly observed upon molding the HS-powder as HS-film. This indicates that the large interparticle space between neighboring nanospheres is efficiently reduced by high-pressure extrusion, which is in good agreement with the observation of the SEM images.[32] Correspondingly, a quick drop of the BJH pore-size distribution is observed at the diameter over 15 nm, suggesting that the mesopores formed by nanospheres accumulation are virtually removed (Figure 2b). In contrary, no evident difference in isotherm could be discovered between the HS-film and the HS-powder below the region of 0. 85 P/P^0, which directly indicates that the nanoarchitecture of the HS nanospheres in particular the hollow framework with the microporous shells, are perfectly preserved in the HS-film without any collapse (Figure 2).[30] This important finding means that the unique nanostructural properties of the HS can be exploited for the fabrication of solid-like electrolytes that is, employing the empty hollow space for liquid loading and the microporous silica shells for liquids confining. It should be pointed out that in principle the abundant micropores across the silica shells should work with a similar function of capillary action to keep the liquids from leaking and evaporating, making the full liquid-soaked HS-powder and HS-film still in apparent dry solid-state.[35] To demonstrate this conclusion, an additional experiment is carried out as described in the Supporting Information. In Figure S3, the HS-powder fully soaked with organic liquid electrolytes still remains in dry solid-state, while the solid silica spheres (ca. 30 nm) exhibit a typical behavior of gel materials, visually highlighting the importance of hollow structures for electrolyte fabrication. The corresponding textural parameters calculated from N_2-sorption isotherms are listed in Supporting Information Table S1.

Because of the good chemical compatibility and the high Li ionic conductivity, two typical liquid-state electrolytes, namely, $LiPF_6$/ethylene carbonate−dimethyl carbonates−diethyl carbonates ($LiPF_6$/EC-DMC-DEC) and lithium bis-(trifluoromethanesulfonyl)imide/ethylmethylimidazolium bis-(trifluoro methanesulfonyl)imide (LiTFSI/EMIm-TFSI), were employed as the Li^+ conductive media for the construction of solid-like electrolytes. The resultant samples are denoted as HS-

DOI: 10.1021/acs.nanolett.5b00739
Nano Lett. 2015, 15, 3398−3402

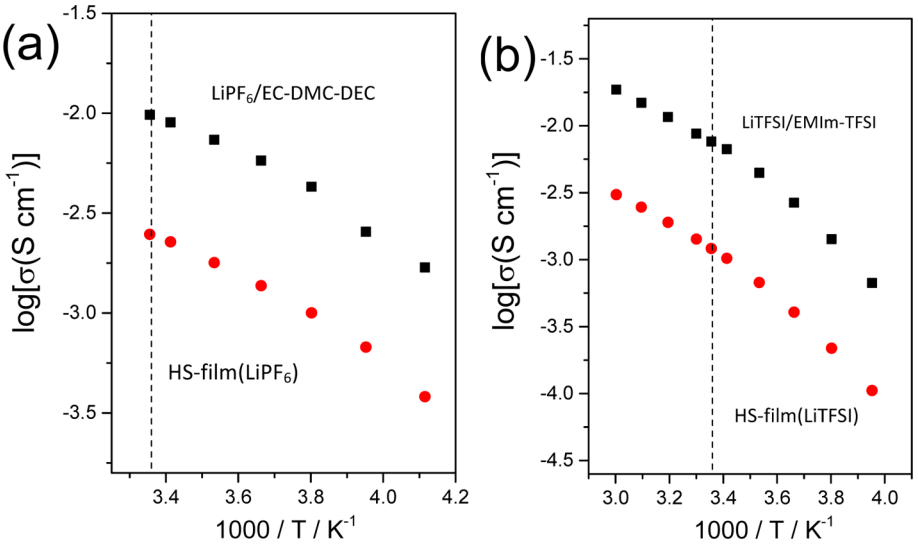

Figure 3. Temperature dependence of ionic conductivities of HS-film($LiPF_6$) (a) and HS-film(LiTFSI) (b). Their corresponding liquid-state counterparts are selected as references. Dash lines here indicate the position of room temperature.

film($LiPF_6$) and HS-film(LiTFSI), respectively. Interestingly, the opaque HS-film becomes optical transparent after fully soaked with liquid media, directly demonstrating that the empty cavities have been fully filled with liquids to allow visible light to pass through (Scheme 1). For 0.1 g of HS-film, the loading amount of $LiPF_6$/EC-DMC-DEC and LiTFSI/EMIm-TFSI is determined as 0.073 and 0.092 g, reaching a degree of volume filling as high as 96.8 and 92.9%, respectively (Supporting Information Table S1). To better demonstrate that the liquids are primarily confined in the empty hollow spheres rather than the interparticle voids, HS-powder filled with LiTFSI/EMIm-TFSI (denoted as HS-powder(LiTFSI)) is subjected to N_2-sorption characterization. In Figure 2, the N_2 uptake below the region of 0. 85 quenches quickly, while the hysteresis loop originating from the accumulation of nanospheres is still present in the higher P/P^0 region. This observation suggests that the inner space of the hollow spheres has been already occupied by ionic liquid molecules but the interparticle voids are still empty. In comparison, the empty cavities in the HS-film(LiTFSI) have been completely removed by the inclusion of ionic liquid molecules (Figure 2).

The ionic conductivities of the HS-film($LiPF_6$) and the HS-film(LiTFSI) were characterized as a function of temperature. In Figure 3, the ionic conductivities of both HS-film($LiPF_6$) and HS-film(LiTFSI) exhibit a typical Arrhenius-type behavior, and their activation energies (E_a) are calculated as 0.23 and 0.33 eV, respectively (Supporting Information Figure S4). These E_a values are almost the same with the data of their corresponding liquid-state counterparts (0.22 and 0.32 eV), demonstrating that the fundamental ion transport properties remain unchanged within HS-film.[23,24] As a result of strong nanoconfinement to well preserve liquids in hollow spheres, a slight drop of ionic conductivities is discovered for solid-like electrolytes.[23,35] For example, the room-temperature conductivities of the HS-film($LiPF_6$) and the HS-film(LiTFSI) are determined as 2.5 and 1.2 mS cm^{-1}, which are only less than 1 order of magnitude lower than their respective liquids (10 and 7.6 mS cm^{-1}) but still meet the requirement for a normal battery operation (1 mS cm^{-1} at ambient temperature).[22] These typical liquid-like ionic conductivities imply that the hollow nanoarchitectures are a promising host for liquid electrolytes loading to afford superior conductivity.

To evaluate the mechanical stability of the HS-film against Li dendrites, a time-dependent voltage profile generated by periodically charged and discharged with a constant current density was performed on a symmetric Li||Li cell assembled by HS-film($LiPF_6$) electrolyte (Figure 4 inset), mimicking the

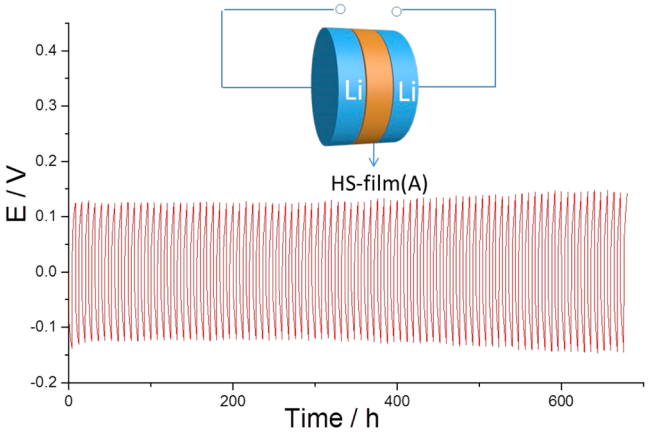

Figure 4. Voltage profiles for lithium plating/striping experiment as a function of time for symmetric lithium coin cells cycled at a fixed current density of 0.16 mA cm^{-2}. Inset is the schematic representation of Li|HS-film ($LiPF_6$)|Li symmetric cell.

operation in Li metal batteries. In Figure 4, a stable voltage profile without any voltage drop is realized on Li|HS-film ($LiPF_6$)|Li symmetric cell, as cycling the cell under a high current density of 0.16 mA cm^{-2} for 685 h and 0.32 mA cm^{-2} for 100 h (Supporting Information Figure S5). When the current density is increased to 1.0 mA cm^{-2}, there is no evidence of the cell failure caused by a short-circuit from dendrite growth (Supporting Information Figure S5). This suggests that the HS-film is mechanically robust to overcome the dendrite problems, stabilizing the cell system from failure by an internal short-circuit in a long-term operation.[23−25,36]

In conclusion, a promising synthetic strategy for the fabrication of solid-like electrolytes with superior ionic

DOI: 10.1021/acs.nanolett.5b00739
Nano Lett. 2015, 15, 3398−3402

conductivities has been successfully developed by entirely utilizing the unique nanostructure-dependent advantages of the HS-film architures.[26,28−30] The well-preserved hollow spheres with the microporous silica shells in the HS-film exhibit a rather strong nanoconfinement behavior to keep liquids in empty cavities,[35] while the HS arrays in a close packing can function as a mechanics-strong separator to efficiently block the Li dendrites from short-circuiting the cell system during repeated charge−discharge cycling.[23,34] After fully soaked with liquid-state electrolytes, for example $LiPF_6$/EC-DMC-DEC and LiTFSI/EMIm-TFSI, the resultant HS-film($LiPF_6$) and the HS-film(LiTFSI) achieve room-temperature conductivities as high as 2.5 and 1.2 mS cm^{-1}, respectively, although they still remain in dry solid-state. In a symmetric lithium/lithium cell, these solid-like electrolytes demonstrate a robust performance against shorting from Li dendrites. Currently, further optimizing the solid-like electrolyte system for the assembly of lithium metal battery is ongoing, including the chemical functionalization of silica shells with nitrile-rich molecules to prevent the invasion of polysulfide species and the nano-engineering of the HS-film with favorable electrochemical properties for the battery operation.[26,37] Furthermore, the high flexibility and compatibility of the HS-film scaffolds, in principle, enables broad tunability to choose desired liquids for the fabrication of other kinds of solid-like electrolytes, such as liquid-state electrolytes containing Na^+, Mg^{2+}, or Al^{3+} as conductive media, providing promising alternative strategy for the development of next generation rechargeable batteries.[1,2,38]

■ ASSOCIATED CONTENT

Supporting Information

Experimental section, Table S1, and Figures S1−5. This material is available free of charge via the Internet at http://pubs.acs.org.

■ AUTHOR INFORMATION

Corresponding Author

*E-mail: dais@ornl.gov.

Notes

The authors declare no competing financial interest.

■ ACKNOWLEDGMENTS

This research was supported by the U.S. Department of Energy's Office of Science, Office of Basic Energy Sciences, Materials Sciences and Engineering Division. TEM (J.C.) and SEM (D.K.H.) experiments were conducted at the Center for Nanophase Materials Sciences, which is a DOE Office of Science User Facility. J.Z. thanks Lihua Lin for his help with data processing. S.D. and M.P.P. thank Edgar Lara-Curzio for his help with nanoindentation measurements.

■ REFERENCES

(1) Armand, M.; Tarascon, J.-M. *Nature* **2008**, *451*, 652−657.
(2) Tarascon, J.-M.; Armand, M. *Nature* **2001**, *414*, 359−367.
(3) Goodenough, J. B.; Abruña, H. D.; Buchanan, M. V. Report of the Basic Energy Sciences Workshop on Electrical Energy Storage, April 2−4, 2007; http://web.anl.gov/energy-storage-science/publications/EES_rpt.pdf.
(4) Whittingham, M. S. *Chem. Rev.* **2004**, *104*, 4271−4302.
(5) Ji, X.; Lee, K. T.; Nazar, L. F. *Nat. Mater.* **2009**, *8*, 500−506.
(6) Bruce, P. G.; Freunberger, S. A.; Hardwick, L. J.; Tarascon, J.-M. *Nat. Mater.* **2012**, *11*, 19−29.
(7) Manthiram, A.; Fu, Y.; Chung, S.-H.; Zu, C.; Su, Y.-S. *Chem. Rev.* **2014**, *114*, 11751−11787.
(8) Wu, H.; Zheng, G.; Liu, N.; Carney, T. J.; Yang, Y.; Cui, Y. *Nano Lett.* **2012**, *12*, 904−909.
(9) Park, J.-B.; Hassoun, J.; Jung, H.-G.; Kim, H.-S.; Yoon, C. S.; Oh, I.-H.; Scrosati, B.; Sun, Y.-K. *Nano Lett.* **2013**, *13*, 2971−2975.
(10) Bhattacharyya, R.; Key, B.; Chen, H.; Best, A. S.; Hollenkamp, A. F.; Grey, C. P. *Nat. Mater.* **2010**, *9*, 504−510.
(11) Lu, Y.; Tu, Z.; Archer, L. A. *Nat. Mater.* **2014**, *13*, 961−969.
(12) Ding, F.; Xu, W.; Graff, G. L.; Zhang, J.; Sushko, M. L.; Chen, X.; Shao, Y.; Engelhard, M. H.; Nie, Z.; Xiao, J.; Liu, X.; Sushko, P. V.; Liu, J.; Zhang, J.-G. *J. Am. Chem. Soc.* **2013**, *135*, 4450−4456.
(13) Liu, N.; Lu, Z.; Zhao, J.; McDowell, M. T.; Lee, H.-W.; Zhao, W.; Cui, Y. *Nat. Nanotechnol.* **2014**, *9*, 187−192.
(14) Suo, L.; Hu, Y.-S.; Li, H.; Armand, M.; Chen, L. *Nat. Commun.* **2013**, *4*, 1481.
(15) McDowell, M. T.; Lee, S. W.; Ryu, I.; Wu, H.; Nix, W. D.; Choi, J. W.; Cui, Y. *Nano Lett.* **2011**, *11*, 4018−4025.
(16) Wang, H.; Yang, Y.; Liang, Y.; Robinson, J. T.; Li, Y.; Jackson, A.; Cui, Y.; Dai, H. *Nano Lett.* **2011**, *11*, 2644−2647.
(17) Kamaya, N.; Homma, K.; Yamakawa, Y.; Hirayama, M.; Kanno, R.; Yonemura, M.; Kamiyama, T.; Kato, Y.; Hama, S.; Kawamoto, K.; Mitsui, A. *Nat. Mater.* **2011**, *10*, 682−686.
(18) Thangadurai, V.; Narayanan, S.; Pinzaru, D. *Chem. Soc. Rev.* **2014**, *43*, 4714−4727.
(19) Lu, Y.; Das, S. K.; Moganty, S. S.; Archer, L. A. *Adv. Mater.* **2012**, *24*, 4430−4435.
(20) Srivastava, S.; Schaefer, J. L.; Yang, Z.; Tu, Z.; Archer, L. A. *Adv. Mater.* **2014**, *26*, 201−234.
(21) Khurana, R.; Schaefer, J. L.; Archer, L. A.; Coates, G. W. *J. Am. Chem. Soc.* **2014**, *136*, 7395−7402.
(22) Wiers, B. M.; Foo, M.-L.; Balsara, N. P.; Long, J. R. *J. Am. Chem. Soc.* **2011**, *133*, 14522−14525.
(23) Tu, Z.; Kambe, Y.; Lu, Y.; Archer, L. A. *Adv. Energy Mater.* **2014**, *4*, 1300654.
(24) Park, K.; Cho, J. H.; Shanmuganathan, K.; Song, J.; Peng, J.; Gobet, M.; Greenbaum, S.; Ellison, C. J.; Goodenough, J. B. *J. Power Sources* **2014**, *263*, 52−58.
(25) Ansari, Y.; Guo, B.; Cho, J. H.; Park, K.; Song, J.; Ellison, C. J.; Goodenough, J. B. *J. Electrochem. Soc.* **2014**, *161*, A1655−A1661.
(26) Lou, X. W.; Archer, L. A.; Yang, Z. *Adv. Mater.* **2008**, *20*, 3987−4019.
(27) Lee, J.; Kim, S. M.; Lee, I. S. *Nano Today* **2014**, *9*, 631−667.
(28) Sun, J.; Zhang, J.; Zhang, M.; Antonietti, M.; Fu, X.; Wang, X. *Nat. Commun.* **2012**, *3*, 1139.
(29) Qiao, Z.-A.; Zhang, P.; Chai, S.-H.; Chi, M.; Veith, G. M.; Gallego, N. C.; Kidder, M.; Dai, S. *J. Am. Chem. Soc.* **2014**, *136*, 11260−11263.
(30) Zhang, J.; Chai, S.-H.; Qiao, Z.-A.; Mahurin, S. M.; Chen, J.; Fang, Y.; Wan, S.; Nelson, K.; Zhang, P.; Dai, S. *Angew. Chem., Int. Ed.* **2015**, *54*, 932−936.
(31) Yang, J.; Lee, J.; Kang, J.; Lee, K.; Suh, J.-S.; Yoon, H.-G.; Huh, Y.-M.; Haam, S. *Langmuir* **2008**, *24*, 3417−3421.
(32) Li, X.; Liu, X.; Ma, Y.; Li, M.; Zhao, J.; Xin, H.; Zhang, L.; Yang, Y.; Li, C.; Yang, Q. *Adv. Mater.* **2012**, *24*, 1424−1428.
(33) Yin, J.; Retsch, M.; Lee, J.-H.; Thomas, E. L.; Boyce, M. C. *Langmuir* **2011**, *27*, 10492−10500.
(34) W. N, S., Jr; Pulskamp, J.; Gianola, D. S.; Eberl, C.; Polcawich, R. G.; Thompson, R. J. *Exp. Mech.* **2007**, *47*, 649−658.
(35) Fichtner, M. *Phys. Chem. Chem. Phys.* **2011**, *13*, 21186−21195.
(36) Qian, J.; Henderson, W.; Xu, W.; Bhattacharya, P.; Engelhard, M.; Borodin, O.; Zhang, J. *Nat. Commun.* **2015**, *6*, 3762.
(37) Ma, L.; Zhuang, H.; Lu, Y.; Moganty, S. S.; Hennig, R. G.; Archer, L. A. *Adv. Energy Mater.* **2014**, *4*, 1400390.
(38) Yabuuchi, N.; Kubota, K.; Dahbi, M.; Komaba, S. *Chem. Rev.* **2014**, *114*, 11636−11682.

DOI: 10.1021/acs.nanolett.5b00739
Nano Lett. 2015, 15, 3398−3402